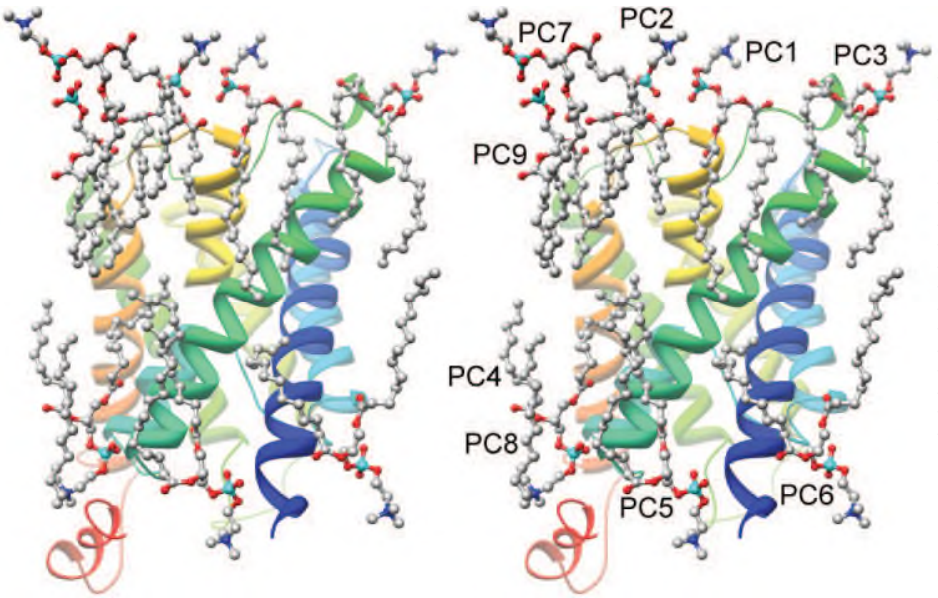

Nature. 2005 December 1; 438(7068): 633–638.

2B6P, 2B6O, 1YMG

Extracellular AQP0

H1 – blue
H2 – light blue
HB - cyan
H3 – light green
H4 – green
H5 – yellow
HE - gold
H6 – orange
CT – red
Cytopasm

Figure 7: Lipids surrounding the AQP0 tetramer mediate the crystal contacts. Horizontal section through an **AQP0** tetramer (blue) showing one of the water molecules in the pore (red) and the tightly packed acyl chains of the surrounding shell of lipid molecules (**yellow**).

Supplementary **2B6P pH=6.5** Table1: Crystallographic statistics of non junctional **AQP0** (X-ray).

None of the **AQP** 3D crystals examined so far contain **lipid**s, and 2D crystals of **AQP**s can form with a variety of different **lipid**s, suggesting that **AQP**s have neither a requirement for specific **lipid**s nor high-affinity **lipid** binding sites **hydrophobic**. Nevertheless, our density map revealed that between the **AQP**0 **tetramer**s are horseshoe-shaped features characteristic of **lipid** molecules (Fig. 4a). Indeed, close inspection revealed that **lipid**s **bridge-hydrophobic** all the contacts between **tetramer**s within a layer and that the **tetramer**s have **essentially hydrophobic** lateral **interaction**. In composite omit maps, we could identify **nine lipid**s per **AQP**0 **monomer**, which we modeled as complete or partial molecules of **dimyristoyl phosphatidyl choline** (**DMPC**, the **lipid** used for 2D crystallization) (Fig. 4a). **Phospholipid** head**group**s have a chiral center at **C2** of the glycerol, and the **DMPC** we used is a racemic mixture. Density is weak or absent at most **C2** positions in our map, and often at the attached ester **group** as well, suggesting that there is little or no selectivity for the biological enantiomer. Very strong density for the **phosphate group**s, weaker but well defined density for the **trimethyl amine group**s of the **cholines**, and unambiguous density for the **acyl chain**s allowed us to build and refine a model in which we chose an enantiomer for each **lipid** more or less arbitrarily. We have not yet attempted to refine the **two** alternatives with 50% occupancy each. We have annotated these **lipid**s as **PC**1 to **PC**9 (Fig. 4b; Suppl. Fig. 6). **PC**1 to **PC**7 have extensive protein contacts and appear to represent "annular **lipid**s" immediately adjacent to a **membrane** embedded protein. **PC**8 and **PC**9 are not in contact with protein and thus represent bulk **lipid**s. A detailed description of protein-**lipid** contacts is provided in Supplementary Materials. As **AQP**0 has no tight **lipid** binding sites, **interaction**s between the annular **lipid**s and the **AQP**0 subunits are likely to represent the kind of contacts that occur between any **membrane** protein and the **lipid**s surrounding it.

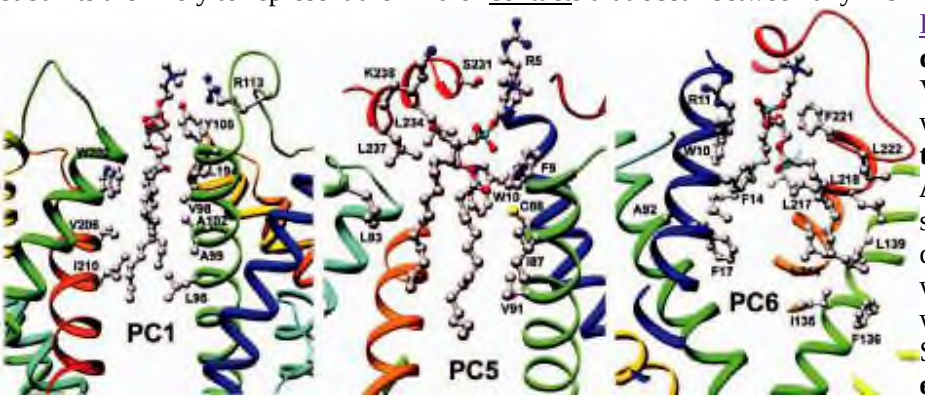

Figure 4**: Lipid-protein interactions in double-layered AQP0 2D crystals. a.** Vertical slab through the 2Fo-Fc density map with modelled **lipid** molecules, revealing the **two lipid bilayer**s in the double-layered **AQP**0 2D crystal. **b**. The **nine lipid**s surrounding an **AQP**0 **monomer** in the 2D crystal. **Lipid**s **PC1** to **PC7** are annular **lipid**s, whereas lipids **PC8** and **PC9** are bulk **lipid**s with no direct protein contacts. See Supplementary Figure 6 for a stereo view. **c – e.** Three examples of lipids sandwiched in between two **AQP**0 molecules. The **acyl chain**s of **PC1** adopt a closed (**c**), those of **PC5** a slightly splayed (**d**), and those of **PC6** a widely splayed conformation (**e**).

Annular **lipid**s must adapt to the irregular surface of a **transmembrane** protein to create a smooth interface for bulk **lipid**s. This fit limits the mobility (and perhaps the chemistry) of annular **lipid**s, as their conformations are partially defined by the

protein surface. In our 2D arrays, most of the annular **lipid**s are sandwiched between **two tetramer**s and thus mediate lattice **interact**ions (Suppl. Fig. 7). This packing further restricts their conformations. The **cell** dimensions of our reconstituted **junction**s are the same as those in thin **junction**s between **lens fibre cell**s [28]. We therefore suggest that the **lipid**-protein **interact**ions we observe in our 2D crystals with the artificial **lipid DMPC** are representative of those formed by **AQP**0 **tetramer**s with native **lipid**s in **lens fibre cell membran**es.

The **lipid**s form a one-molecule wide annular shell around the protein. The positions of the head**group**s vary by only ±2 Å in the direction perpendicular to the **membran**e plane, with a separation of about **34 Å** from **phosphate** to **phosphate**. The dimensions of the **bilayer** correspond closely to those of fully hydrated, fluid phase **DMPC** [29]. A hydrated network of **hydrogen bond**s and salt **bridge**s holds the **lipid phosphate**s in place. Protein **group**s **interact**ing with **phosphate**s include **three Arginine** side **chain**s, a **tyrosine** hydroxyl that mediates one of the **Arginine** contacts, a **lysine**, a **tryptophan** indole **nitrogen**, a **glutamine** side-**chain** amide, and at least one main-**chain** amide. Similar **interact**ions have been described for specifically bound **lipid**s [30].

Acyl chains fill the gaps between adjacent **tetramer**s. Their conformations clearly adapt to the knobs and grooves of the apposed hydrophobic protein surfaces. Figures 4c-e illustrate **three** examples. **PC**1 in the **extracell**ular leaflet is the best ordered of the **nine DMPC** molecules. Its **acyl chain**s are nearly fully extended, packed against those of **PC**2 and **PC**3 and sandwiched between five **non**-polar side **chain**s from one **AQP**0 and **three** from the other. **PC**5 in the **cytoplasm**ic leaflet has somewhat less extended **acyl chain**s. The **phosphate** receives a **hydrogen bond** from the indole **nitrogen** of **Trp10** and **Lys238** (as well as the poorly ordered **N-termin**al segment) of an adjacent subunit. The **acyl chain**s, packed between those of **PC**4 and **PC**6, contact four hydrophobic side **chain**s from one subunit (including the hydrophobic face of **Trp10**) and **three** from another. **PC**6, also in the **cytoplasm**ic leaflet, has widely splayed **acyl chain**s, separated by side **chain**s from the **two** apposed **AQP**0 molecules. **Phe14** of one molecule and **Leu217** of another are in van der Waals contact through the gap: the only direct **interact**ion between **tetramer**s within a layer.

PC8 and **PC**9 lie near the fourfold axis. They do not contact protein and thus represent bulk **lipid**s. Neither is as well ordered as the annular **lipid**s. Indeed, **PC**8 (in the **cytoplasm**ic leaflet) is probably only statistically ordered (**two**, rather than **four**, molecules about a fourfold), as there is space for only one of the **two acyl chain**s and no density for the head**group**. The head**group** of **PC**9 lies about 3 Å closer to the midplane of the **bilayer** than those of the four other **extracell**ular leaflet **lipid**s; the **bilayer** thickness may therefore be influenced by adjacency to the protein. **2B6P pH=6.5** non junltional **2B6O pH=10.5**

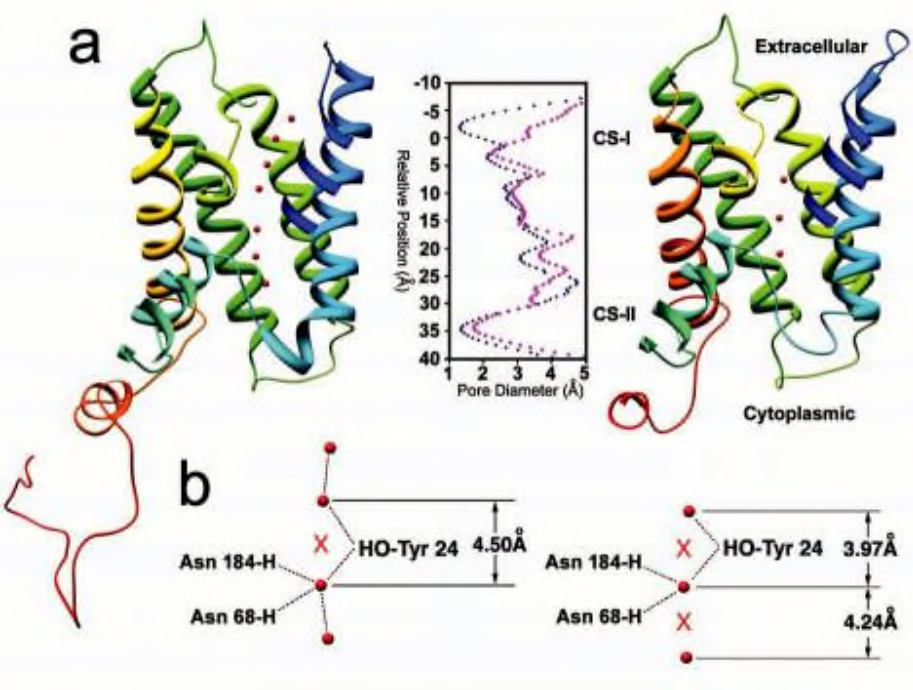

Figure 3: The **water pore in AQP0. a.** The **por**e in **non-junction**al **AQP**0 (left) contains **seven water** molecules (red spheres), while the **por**e in **junction**al **AQP**0 contains only **three water** molecules (right). Calculated **por**e profiles (middle) corroborate that the **por**e.

In our initial re**por**t of the closed **water por**e in **junction**al **AQP**0 [7], we proposed that **AQP**0 and other **Aquaporin**s may be in a dynamic equilibrium between an open and a closed **por**e conformation. We also suggested that **por**e closure may be triggered by the stabilisation of an alternative conformation of **Arg187** (part of the **ar/R** constriction site) seen in the structure of **junction**al **AQP**0. A recent molecular dynamics study sup**port**s this notion, as it showed that **Arg189** in **AQP**Z (corresponding to **Arg187** in **AQP**0) could adopt **two** conformations [20]. The "UP" state, which is seen in most **AQP** crystal structures, had an open **por**e, filled by a continuous single file of **water**. The "DOWN" state, seen in our structure of **junction**al **AQP**0, had a **por**e completely blocked by the **Arg** side **chain**, and prolonged blockage resulted in loss of all **water** molecules from the **por**e. While attractive, a conformational switch of the **Arginine** in the **ar/R** constriction site cannot be the only mechanism for **AQP** gating, because **Arg187** is in the "DOWN" state not only in our closed, **junction**al **AQP**0 but also in the open, **non-junction**al **AQP**0 structure [8]. The main difference between the open and closed **por**e lies in the conformation of the side **chain** of **Met176** (see above), a residue not present in **AQP**Z.

The distances between the **three water** molecules **(≥4 Å)** in the closed **por**e are too long for **hydrogen bond**ing (Fig. 3b, right; Suppl. Fig. 5, right). The **water** coordinated to the Asn residues of the **two NPA** motifs donates a **hydrogen bond** to the hydroxyl **group** of **Tyr24**, which in turn donates a **hydrogen bond** to the **water** molecule in the **extracell**ular half of the **water** pathway (Fig. 3b, right; Suppl. Fig. 5, right). The corresponding **two water** molecules in the open **water por**e of **non-junction**al **AQP**0 have the same **hydrogen bond**ing pattern (Fig. 3b, left; Suppl. Fig. 5, left), and all the other **water** molecules are in **hydrogen-bond**ing distance to each other. "**Phenol**ic barrier created by **Tyr24**, a residue not seen in the other known **AQP** structures, may be responsible for the poor **water** conductance of **AQP**0 as compared to other **AQP**s, which contain a continuous line of **hydrogen-bond**ed **water** molecules. The space occupied by **Tyr24** may also explain why the open **AQP**0 **por**e contains only **seven water** molecules while molecular dynamics studies showed **eight water**s in **AQP**1 [21,22] and **AQP**Z [20] and **nine** in **GlpF** [23].

AQP0 **water** conductance is **pH**-dependent with a maximum at **pH 6.5** and only about half the activity at **pH 10.5** [12]. These conductance characteristics are not changed by proteolytic cleavage of **AQP**0 [24]. As our structure, obtained with the double-layered 2D crystals grown at **pH 6** [7], reveals fewer **water** molecules in the **por**e than the structure determined from the 3D crystals grown at **pH 10.5** [8], **por**e closure appears to be a result of **junction** formation, not **pH** shift.

OPEN 2B6P pH=6.5 non junltional

```
REMARK 525    HOH A 328        DISTANCE =  5.22 ANGSTROMS                          2B6P
REMARK 525    HOH A 340        DISTANCE =  6.88 ANGSTROMS
REMARK 525    HOH A 347        DISTANCE =  6.00 ANGSTROMS
REMARK 525    HOH A 348        DISTANCE =  5.04 ANGSTROMS
REMARK 525    HOH A 362        DISTANCE =  5.54 ANGSTROMS
REMARK 525    HOH A 376        DISTANCE =  5.45 ANGSTROMS
HELIX    1   1 PHE A    9  LEU A   32  1                                   24
HELIX    2   2 GLY A   37  GLY A   64  1                                   28
HELIX    3   3 ASN A   68  GLY A   78  1                                   11
HELIX    4   4 SER A   82  THR A  108  1                                   27
HELIX    5   5 SER A  126  ASP A  150  1                                   25
HELIX    6   6 SER A  159  GLY A  180  1                                   22
HELIX    7   7 ASN A  184  ARG A  196  1                                   13
HELIX    8   8 TRP A  202  PHE A  221  1                                   20
HELIX    9   9 SER A  229  LEU A  237  1                                    9
```

junltional **2B6O pH=10.5** half **OPEN**

```
REMARK 525    HOH A 281        DISTANCE =  7.45 ANGSTROMS                          2B6O
REMARK 525    HOH A 282        DISTANCE =  5.39 ANGSTROMS
REMARK 525    HOH A 305        DISTANCE =  7.20 ANGSTROMS
REMARK 525    HOH A 314        DISTANCE =  5.12 ANGSTROMS
REMARK 525    HOH A 346        DISTANCE =  9.27 ANGSTROMS
HELIX    1   1 ARG A    5  LEU A   32  1                                   28
HELIX    2   2 LEU A   39  VAL A   59  1                                   21
HELIX    3   3 GLY A   60  ILE A   62  5                                    3
HELIX    4   4 ASN A   68  GLY A   78  1                                   11
HELIX    5   5 SER A   82  THR A  108  1                                   27
HELIX    6   6 SER A  126  TYR A  149  1                                   24
HELIX    7   7 SER A  159  MET A  176  1                                   18
HELIX    8   8 ASN A  184  ARG A  196  1                                   13
HELIX    9   9 TRP A  202  PHE A  221  1                                   20
HELIX   10  10 SER A  229  LEU A  234  1                                    6
HELIX   11  11 SER A  235  LEU A  237  5                                    3
SITE     1 AC1  6 ARG A 196  MC3 A 269  MC3 A 270  MC3 A 272
SITE     2 AC1  6 HOH A 273  HOH A 304
SITE     1 AC2  8 ALA A 102  VAL A 103  TYR A 105  SER A 106
SITE     2 AC2  8 MC3 A 270  HOH A 291  HOH A 301  HOH A 327
SITE     1 AC3  9 LEU A  83  LEU A  84  ILE A  87  VAL A  90
SITE     2 AC3  9 VAL A  91  LEU A  94  LYS A 238  MC3 A 267
SITE     3 AC3  9 MC3 A 271
SITE     1 AC4  8 ARG A   5  SER A   6  PHE A   9  TRP A  10
SITE     2 AC4  8 LEU A  84  CYS A  88  MC3 A 266  MC3 A 272
SITE     1 AC5  4 ALA A   7  TRP A  10  ARG A  11  PHE A  14
SITE     1 AC6  2 MC3 A 264  MC3 A 272
SITE     1 AC7  8 LEU A  95  TYR A 105  ILE A 193  LEU A 194
SITE     2 AC7  8 ARG A 196  MC3 A 264  MC3 A 265  HOH A 326
SITE     1 AC8  1 MC3 A 266
SITE     1 AC9  3 MC3 A 264  MC3 A 267  MC3 A 269
```